Supplementary Materials for:

Distinct multisensory perceptual processes guide enhanced auditory recognition memory in older cochlear implant users

Jan-Ole Radecke, Irina Schierholz, Andrej Kral, Thomas Lenarz, Micah M.Murray and Pascale Sandmann

Supplementary Materials

A. CI Electrical Artifact and Different Trial Numbers Did Not Affect Signal-to-Noise Ratio

The primary CI electrical artifact components identified by the ICA, showed a time course with a clear peak in response to the auditory stimulus onset (0-50 ms) and a smaller and inverted peak in response to the stimulus offset (500-550 ms after stimulus onset) (Suppl. Fig. 1A). The CI processing of naturalistic sounds with complex temporal dynamics, showed the largest impact of the CI electrical artifact on ERP topographies right after the onset of auditory stimulation (Viola et al., 2011). The corresponding component topographies consistently revealed a voltage distribution with a lateral centroid on the side of stimulation (Suppl. Fig. 1B). In some CI users, the ICA revealed additional sustained activation patterns that were reflected by additional independent components. Overall, 21.6 % (± 3.5 %; CI) and 19 % (± 0.3 %; NH) of the initial independent components were rejected on average for CI users and NH controls, respectively (including artifacts related to the CI in CI users and to eye blinks, eye movements, muscle activity, and heart-beat in both groups).

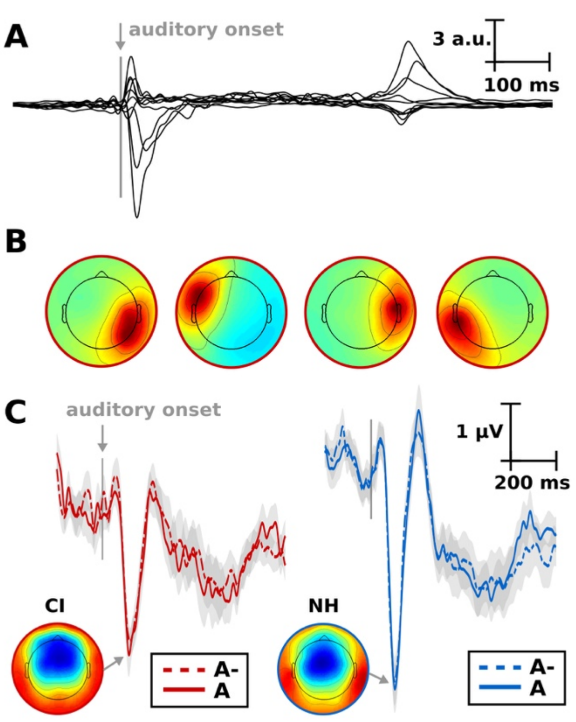

Supplementary Figure 1. A) Electrical CI-artifacts, evoked by auditory stimuli were evaluated for 10 CI users in a piloting data analysis of the presented study. Independent component time-series of primary electrical CI artifacts of CI users are displayed, averaged across trials for each subject and time-locked to the auditory onset. Auditory stimulus onset and offset evoked large responses that varied in amplitude across subjects due to the intracochlear electrode placement and individual technical implant details. B) Independent component topographies for the same CI-artifacts are shown for four exemplary subjects to illustrate the typical ellipsoid voltage distribution, lateralized to the side of the implant. C) Auditory ERPs for stimulus conditions A (solid lines) and A- (dashed lines) after the artifact correction using ICA for both CI users (red lines) and NH listeners (blue lines). Clear auditory ERPs and central N1 topographies were observed in CI users, indicating a sufficient and specific attenuation of the CI-artifact by the independent component analysis.

Due to residual CI artifact or due to a different number of trials that were available for averaging after EEG processing, the signal-to-noise ratio (SNR) of the ERPs might be affected (Clayson et al., 2013). In order to exclude potential confounds of distinct SNRs, an additional analysis was computed. As the auditory N1 component typically yields a large and robust response in CI users (Viola et al., 2011), the SNR was estimated as the ratio between the N1-peak (signal, *S*), detected at a fronto-central electrode cluster, and the standard deviation of the pre-stimulus baseline interval as an estimate of noise (*N*; Debener et al., 2008). SNR estimates were transformed to logarithmic scale ($SNR = 20 \log_{10} \frac{S}{N}$) and compared by separate mixed model repeated-measures ANOVA for initial ERPs, including the factors Group (NH, CI) and initial Stimulus Condition (AVm, A, AVc), as well as for repetition ERPs, including the factors Group (NH, CI) and repetition Stimulus Condition (A+m, A-, A+c). No main effect of Group or Stimulus Condition and no interaction effect, neither for initial nor for repetition ERPs was revealed (Initial: all $p \geq 0.097$; Repetition: all $p \geq 0.538$). This analysis indicates a sufficient signal quality for further analysis of auditory evoked ERPs in the present sample.

B. ERPs and Difference ERPs to Repetition Trials

ERPs to repetition trials were similar across conditions (Supplementary Fig. 2) and no group-specific differences in GFP or GMD were observed ($CI_{A+c\ -\ A+m}$ vs. $NH_{A+c\ -\ A+m}$; Supplementary Fig. 3).

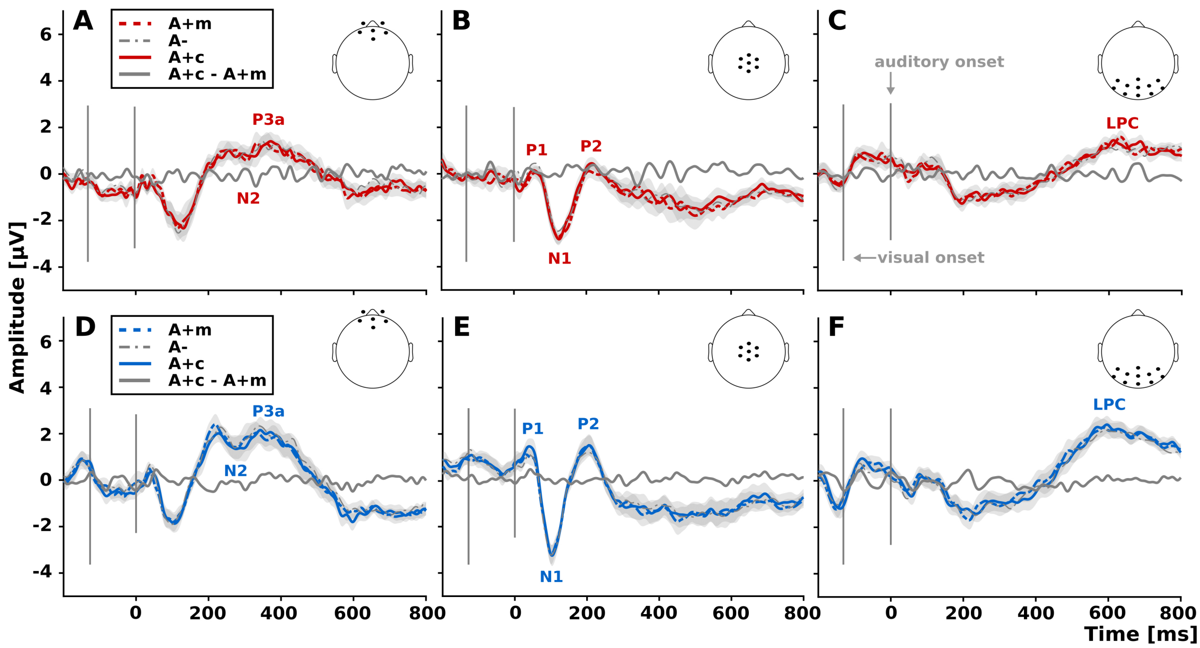

Supplementary Figure 2. ERPs to auditory repetition stimulus conditions (A+m, A-, A+c) for CI users (panels A-C) and NH participants (panels D-F), in a frontal (A, D), a central (B, E) and a parieto-occipital (C, F) electrode cluster, respectively. ERPs to stimulus condition A- are depicted for descriptive reasons, but hardly show any difference, compared the other repetition stimulus conditions (A+m, A+c). The ERPs were not different between CI users and NH listeners and revealed typical components related to activity during a continuous recognition task. Note the typical auditory P1-N1-P2 complex in the central electrode cluster (B, E). For the frontal electrode cluster (A, D), a subtle anterior N2 component was followed by P3a ERP component. An extended LPC was observed in the parieto-occipital electrode cluster (C, F). The statistical analyses revealed no stimulus condition effects for the repetition ERPs. Mean ERPs for the respective stimulus conditions are represented by the colored dashed and solid lines. Grey patches indicate the SEM for each ERP. Solid grey lines represent the difference ERP ($CI_{A+c\ -\ A+m}$ and $NH_{A+c\ -\ A+m}$). Electrode clusters are indicated on a model head, viewed from top.

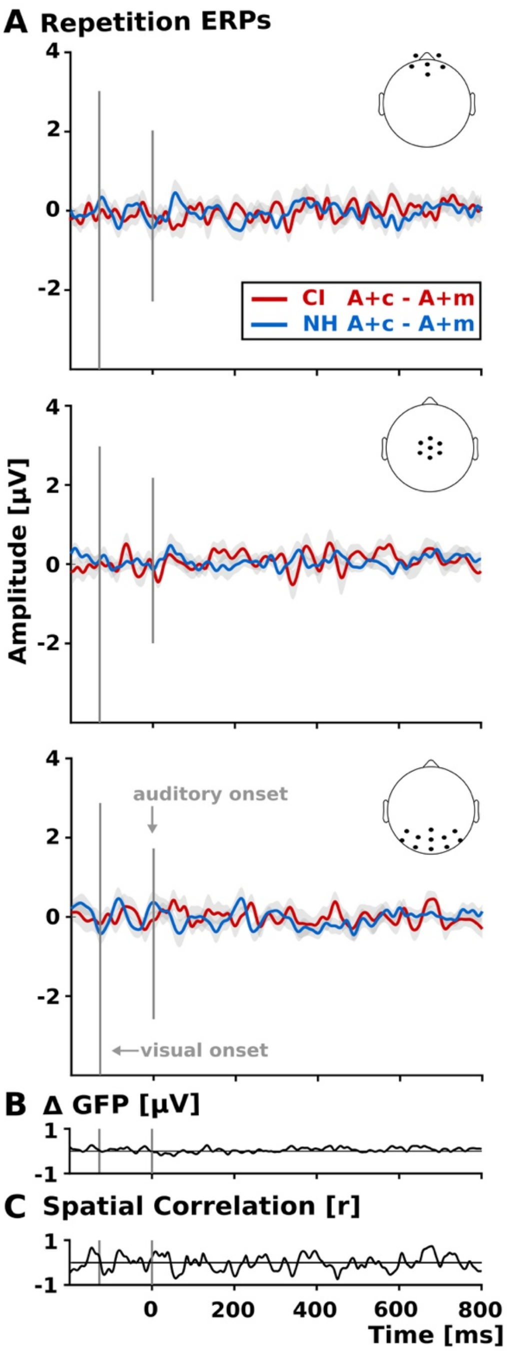

Supplementary Figure 3. Comparison of the difference waves between the two groups. A) Difference ERPs for CI users (red) and NH participants (blue) for auditory repetition stimulus conditions ($CI_{A+c\ -\ A+m}$ and $NH_{A+c\ -\ A+m}$) for three different electrode clusters (from top to bottom: frontal, central, parieto-occipital). Grey patches indicate the SEM for each difference ERP. Electrode clusters are indicated on a model head, viewed from top. B) Global field power was computed for each sample and statistically compared between the two groups by means of a permutation test. The difference of GFPs (Δ GFP) are depicted ($CI_{A+c\ -\ A+m}$ - $NH_{A+c\ -\ A+m}$). No significant differences between groups were observed for the GFP analysis of difference ERPs. C) Sample-wise spatial correlation between difference ERPs ($CI_{A+c\ -\ A+m}$ and $NH_{A+c\ -\ A+m}$). Topographical differences were quantified by computing global dissimilarity for each sample and statistically compared between the two groups by means of a permutation test. No significant differences were revealed for the repetition difference ERPs ($CI_{A+c\ -\ A+m}$ vs. $NH_{A+c\ -\ A+m}$).

C. Sample-wise spatial correlation (200-380 ms)

Sample-wise spatial correlation between template maps (M1, M2, M3) and initial ERPs of each condition (AVc, AVm) and group (CI, NH) illustrate the robust fitting procedure indicating a higher correlation between M1 and ERPs during the AVc condition and M2 and ERPs during the AVm condition (Supplementary Figure 4). As presented in the main manuscript, this dissociation was present only in CI users, not in NH listeners. Likewise, the Stimulus Condition x Template Map interaction (section 3.2.4) indicates distinct neural generators of the template maps M1 and M2 and thus distinct brain networks that characterize specific responses to different stimulus conditions (AVc, AVm). These results are not explained by spurious spatial correlations but reflect the reliable presence of distinct ERP maps that is captured by the occurence counts.

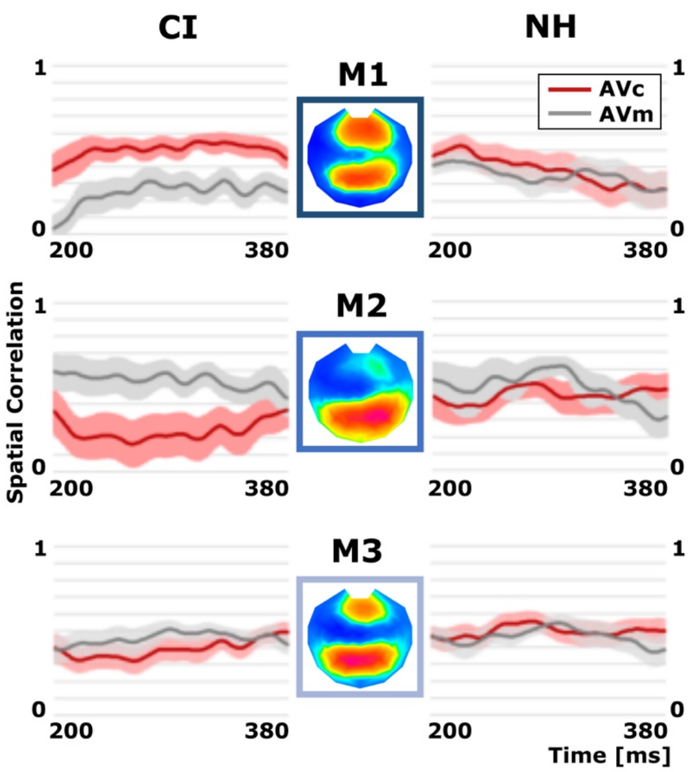

Supplementary Figure 4. Sample-by-sample spatial correlation between the template maps (top to bottom: M1-M3) and the ERPs for conditions AVc (red; M ± SEM) and AVm (grey), separately for CI users (left) and NH listeners (right) and for the 200-380 ms time window. In CI users, template map M1 shows a higher correspondence to ERPs during AVc, whereas M2 shows a higher correlation to ERPs during AVm.

D. Increased Relative Congruency Gain in CI Users

In addition to the evaluation of *absolute d'* scores, *relative* changes in discriminability were computed as $d'_{\text{Change}}(x,y) = 100\ (x/y) - 100$ for 1) the *audio-visual gain* by comparing the congruent audio-visual with the auditory-only recognition condition ($d'_{\text{AVGain}} = d'_{\text{Change}}(d'_{\text{AVc}}, d'_{\text{A}})$), 2) the *congruency gain* by comparing the congruent and the meaningless audio-visual recognition conditions ($d'_{\text{ConGain}} = d'_{\text{Change}}(d'_{\text{AVc}}, d'_{\text{AVm}})$), and 3) the *audio-visual cost* by comparing the meaningless audio-visual with the auditory-only recognition condition ($d'_{\text{AVCost}} = d'_{\text{Change}}(d'_{\text{AVm}}, d'_{\text{A}})$). We computed a mixed-model repeated-measures ANOVA with Relative Gain Condition (d'_{ConGain}, d'_{AVGain} and d'_{AVCost}) as the within-subject factor and Group (CI, NH) as the between-subject factor.

An identified outlier was controlled by computing robust follow-up contrasts (bootstrapped independent samples *t*-tests) between groups for d'_{ConGain}, d'_{AVGain} and d'_{AVCost} and corrected for multiple comparisons using the Bonferroni-Holm correction (Holm, 1979). For the robust *t*-tests, the *z*-transformed test-value and the *p*-values are indicated.

On a descriptive level, both groups showed a considerable *relative gain* in performance when initial auditory object presentations were paired with congruent visual information, in relation to when initial auditory object presentations were purely auditory (d'_{AVGain} CI: 137.3 $\pm$ 33.1%, NH: 39.6 $\pm$ 6.1%) or paired with meaningless visual information ($d'_{ConGain}$ CI: 235.6 $\pm$ 79.9%, NH: 62.6 $\pm$ 10.6%; Fig. 2B). A Group (CI, NH) x Relative Gain Condition ($d'_{ConGain}$, d'_{AVGain}, d'_{AVCost}) repeated-measures mixed-model ANOVA revealed main effects of Group ($F_{1,\ 22} = 17.8$, $p = .027$, $\eta_p^2 = .20$) and Relative Gain Condition ($F_{1.2,\ 26.7} = 10.2$, $p = .002$, $\eta_p^2 = .32$). The Group x Relative Gain Condition interaction resulted in a near-threshold *p*-value ($F_{1.2,\ 26.7} = 3.8$, $p = .055$, $\eta_p^2 = .15$), due to a considerable violation of the sphericity assumption (Sphericity (Mauchly test): $W_2 = .353$, $p < .001$; Greenhouse-Geisser $\varepsilon = .607$). The violation resulted in a strict correction of the degrees of freedom, and a non-significant Greenhouse-Geisser corrected interaction ($F_{1.2,\ 26.7} = 3.8$, $p = .055$, $\eta_p^2 = .15$), while the uncorrected results indicated an interaction (uncorrected degrees of freedom: $F_{2,44} = 3.8$, $p = .03$, $\eta_p^2 = .15$).

Based on the descriptive data (see Figure 2B), an outlier was identified in the group of CI users. In order to evaluate the influence of this outlier on the ANOVA results, a jackknife analysis (leave-one-out) was computed for the repeated-measures mixed-model ANOVA (Suppl. Tab. 1). In this analysis, the ANOVA was computed twelve times (*n* = 12). For every iteration, one CI user and the respective matched control was left out, therefore resulting in *N* = 11 subjects that were included in every iteration *i* of the jackknife analysis. Resulting *F*-values and degrees of freedom (Greenhouse-Geisser corrected, if the sphericity assumption was violated) for the Group x Relative Gain Condition interaction, as well as resulting *p*-values are listed in Supplementary Table 1.

i	F_{df}	*df*		*p*
		df_1	df_2	
1	3.31	1.17	23.3	.076
2	4.32	1.22	24.5	.041
3	2.82	1.21	24.2	.100
4	3.83	1.22	24.4	.055
5	3.15	1.15	23.0	.084
6	3.71	1.20	24.0	.059
7	4.01	1.19	23.8	.050
8	3.10	1.21	24.3	.084
9	3.33	1.21	24.2	.073
10	4.18	1.21	24.3	.045
11	***4.37***	***2***	***40***	***.019***
12	3.40	1.18	23.6	.072

Supplementary Table 1. Results for the Group x Relative Gain Condition interaction effect of the repeated-measures mixed-model ANOVA using the jackknife analysis. For $i = 11$ sphericity assumption was not violated and *F*-value was increased, indicating the respective subject as an outlier that affects the statistical analysis.

The jackknife analysis revealed one participant to bias the outcome of the ANOVA ($i = 11$), with respect to a violation of the sphericity assumption. An average $F_{1.2,24.8} = 3.63$ was observed ($p = .061$; 95% - confidence interval: $F = 3.36 - 3.89$, $p = .052 - .071$). Leaving out this participant increased the *F*-value, while the sphericity assumption was not violated. Importantly, this participant was the same that was descriptively identified as an outlier (Fig. 2B). To validate the specific influence of this one outlier, the jackknife analysis was again performed for the sample, this time excluding the outlier (and the corresponding NH control). Results confirmed a robust Group x Relative Gain Condition interaction effect with an average $F_{2,40} = 4.08$ ($p = .024$; 95% - confidence interval: $F = 3.65 - 4.51$, $p = .017 - .035$).

In sum, we concluded that the Group x Relative Gain Condition interaction effect from the ANOVA was near-threshold, but biased by one outlier. Removing this outlier, resulted in a robust Group x Relative Gain Condition interaction. Due to the small sample size, the outlier was not excluded from the following analysis. Instead robust (bootstrap) follow-up *t*-tests were computed to control the influence of the outlier. Robust follow-up *t*-tests revealed that both the audio-visual gain ($d'_{AVGain} = d'_{Change}(d'_{AVc}, d'_A)$) and the congruency gain ($d'_{ConGain}$ =

$d'_{Change}(d'_{AVc}, d'_{AVm})$) were stronger in CI users when compared with NH listeners (CI(d'_{AVGain}) > NH(d'_{AVGain}): z = -2.8, p = .003; CI(d'_{ConGain}) > NH(d'_{ConGain}): z = -2.1, p = .032). This suggests that CI users show a relatively stronger improvement in auditory object discriminability when the initial auditory presentation was paired with semantically congruent visual information when compared to NH listeners. It has to be noted that this effect seems to be driven specifically by the semantic information of the stimuli and not solely by the presence of additional meaningless visual information per se, as the multisensory facilitation effects were similar for d'_{AVGain} and d'_{ConGain}. No group difference was observed with respect to the audio-visual cost (d'_{AVCost}, p = .083; CI: 60.8 ± 21.2, NH: 20.3 ± 4.9).

However, analyzing the relative gains bears the risk that the observed group differences are driven by baseline imbalances between the CI users and the NH listeners, since CI users show a relatively decreased sensitivity during the auditory condition (d'A), compared to NH listeners (see Figure 2 in the main manuscript). Whether the enhanced gain in CI users is informative despite the observed baseline group-differences remains inconclusive here.

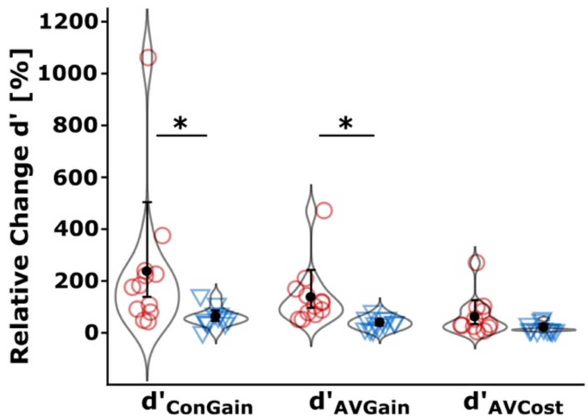

Supplementary Figure 5. Results for the Group x Relative Gain Condition interaction effect of the repeated-measures mixed-model ANOVA using the jackknife analysis. Due to an outlier (see supplementary table 1), non-parametric bootstrap t-tests were applied. The analysis revealed increased congruency gain (d'_{ConGain}) and audio-visual gain (d'_{AVGain}) in CI users, compared to NH listeners.

Supplementary References

Clayson, P.E., Baldwin, S.A., Larson, M.J., 2013. How does noise affect amplitude and latency measurement of event-related potentials (ERPs)? A methodological critique and simulation study. Psychophysiology 50, 174–186. https://doi.org/10.1111/psyp.12001

Debener, S., Hine, J., Bleeck, S., Eyles, J., 2008. Source localization of auditory evoked potentials after cochlear implantation. Psychophysiology 45, 20–24. https://doi.org/10.1111/j.1469-8986.2007.00610.x

Viola, F.C., Thorne, J.D., Bleeck, S., Eyles, J., Debener, S., 2011. Uncovering auditory evoked potentials from cochlear implant users with independent component analysis. Psychophysiology 48, 1470–1480. https://doi.org/10.1111/j.1469-8986.2011.01224.x